Published in final edited form as:
Development. 2006 June ; 133(12): 2419–2433.

Required, Tissue-Specific Roles for Fgf8 in Outflow Tract Formation and Remodeling

Eon Joo Park[1], **Lisa A. Ogden**[2], **Amy Talbot**[2], **Sylvia Evans**[3], **Chen-Leng Cai**[3], **Brian L. Black**[4], **Deborah U. Frank**[2,5], and **Anne M. Moon**[1,2,6,*]

1*Department of Neurobiology and Anatomy, University of Utah School of Medicine, Salt Lake City, UT 84112, USA.*

2*Department of Pediatrics, University of Utah School of Medicine, Salt Lake City, UT 84112, USA.*

3*Institute of Molecular Medicine, Department of Medicine, University of California, San Diego, La Jolla, CA 92093, USA.*

4*Cardiovascular Research Institute, University of California, San Francisco, CA 94143, USA.*

5*Children's Health Research Center, University of Utah School of Medicine, Salt Lake City, UT 84112, USA.*

6*Program in Human Molecular Biology and Genetics, University of Utah School of Medicine, Salt Lake City, UT 84112, USA.*

Abstract

Fibroblast growth factor 8 (Fgf8) is a secreted signaling protein expressed in numerous temporospatial domains that are potentially relevant to cardiovascular development. However, the pathogenesis of complex cardiac and outflow tract defects observed in Fgf8-deficient mice, and the specific source(s) of Fgf8 required for outflow tract formation and subsequent remodeling are unknown. A detailed examination of the timing and location of Fgf8 production revealed previously unappreciated expression in a subset of primary heart field cells; *Fgf8* is also expressed throughout the anterior heart field (AHF) mesoderm and in pharyngeal endoderm at the crescent and early somite stages. We used conditional mutagenesis to examine the requirements for *Fgf8* function in these different expression domains during heart and outflow tract morphogenesis. Formation of the primary heart tube and the addition of right ventricular and outflow tract myocardium depend on autocrine Fgf8 signaling in cardiac crescent mesoderm. Loss of Fgf8 in this domain resulted in decreased expression of the Fgf8 target gene *Erm*, and aberrant production of *Isl1* and its target *Mef2c* in the anterior heart field, thus linking Fgf8 signaling with transcription factor networks that regulate survival and proliferation of the anterior heart field. We further found that mesodermal- and endodermal-derived Fgf8 perform specific functions during outflow tract remodeling: mesodermal Fgf8 is required for correct alignment of the outflow tract and ventricles, whereas activity of Fgf8 emanating from pharyngeal endoderm regulates outflow tract septation. These findings provide a novel insight into how the formation and remodeling of primary and anterior heart field-derived structures rely on Fgf8 signals from discrete temporospatial domains.

Keywords

Fgf8; Cardiovascular; Outflow tract; Congenital heart disease; Truncus Arteriosus; Transposition; 22q11 deletion syndrome; Pharyngeal arches; Neural crest; DiGeorge syndrome

*Author for correspondence (e-mail: anne.moon@genetics.utah.edu)

INTRODUCTION

Cardiogenesis requires specification, differentiation, proliferation and migration of cell populations from diverse sites. Inductive interactions between these populations and regionally-specific transcription factor hierarchies regulate distinct morphogenetic events during heart development; their disruption by mutation or environmental insult usually results in malformations that affect discrete cardiac substructures, leaving the rest of the organ intact (de la Cruz et al., 2001; Harvey, 2002). Given the duration and complexity of heart development, it is not surprising that nearly one percent of humans are born with congenital cardiovascular defects (Creazzo et al., 1998; Harvey, 2002; Olson and Schneider, 2003).

Myocardial precursors leave the primitive streak and reside briefly in a 'cardiac crescent' of bilateral mesoderm where their fate is influenced by adjacent endoderm (Lough and Sugi, 2000; Schultheiss et al., 1995; Yutzey and Kirby, 2002). Clonal analyses revealed that two distinct lineages contribute to the heart (Zaffran et al., 2004), and studies in mouse and chick indicate that crescent mesoderm contains two precursor populations: a 'primary heart field' (PHF) contains the earliest cells to undergo myocardial differentiation, which contribute to the primitive tubular heart and ultimately to the left ventricle (LV), whereas the 'anterior heart field' (AHF) contributes right ventricular (RV) and outflow tract (OFT) myocardium (Buckingham et al., 2005; Zaffran et al., 2004; Cai et al., 2003; de la Cruz et al., 1977; Kelly et al., 2001; Mjaatvedt et al., 2001; Waldo et al., 2001). Although Isl1 is expressed by undifferentiated cells in the AHF, it is also expressed by many LV precursors (Cai et al., 2003) (this manuscript). To date, no proteins have been identified whose expression specifically identifies either field and it is unknown if cells are developmentally restricted within each field. Rather than indicating a distinct molecular identity, the concept of the AHF is currently a teleologic one, reflecting the relative position of a cell in the crescent, the time it contributes to the heart, and its ultimate location within the heart. For clarity, in this manuscript we employ AHF to refer to mesodermal cells residing in the dorsomedial crescent and, subsequently, in anterior splanchnic mesoderm (SM) ventral to the foregut, which are required to form the RV and the OFT.

Transcription factor networks regulate cardiomyocyte specification (Gata4 and Nkx2.5), differentiation (Mef2c), and regional identity within the heart (Brand, 2003; Bruneau, 2002; Cripps and Olson, 2002; Firulli and Thattaliyath, 2002; Fishman and Chien, 1997; Srivastava and Olson, 2000). AHF expression of *Mef2c* is regulated by at least two intronic elements, one of which confers responsiveness to Isl1 and Gata (Dodou et al., 2004) and the other to a Tgfβ/Foxh1/Nkx2.5 pathway (von Both et al., 2004). Although expression of *Mef2c*, *Isl1* and *Foxh1* is not restricted to the AHF, their inactivation primarily disrupts the formation of AHF-derived structures, suggesting that this network regulates the proliferation and survival of undifferentiated AHF cells (Cai et al., 2003; Lin et al., 1997; von Both et al., 2004).

Much less is known about the signaling molecules that trigger cardiomyocyte differentiation, or guide the subsequent formation of cardiac substructures. Endodermal Wnt, Bmp and Fgf signals influence cardiomyocyte differentiation (Brand, 2003), and members of these families have later roles in OFT and valve morphogenesis (Abu-Issa et al., 2002; Armstrong and Bischoff, 2004; Delot et al., 2003; Frank et al., 2002; Liu et al., 2004; Sanford et al., 1997).

Fgf8 and Fgf10 are secreted signaling proteins expressed in the cardiac crescent and in SM (Crossley and Martin, 1995; Kelly et al., 2001). Although *Fgf10*$^{-/-}$ mice survive embryogenesis without cardiac defects (Min et al., 1998; Sekine et al., 1999), germline ablation of *Fgf8* is embryonic lethal (Sun et al., 1999). The complex cardiac and OFT phenotypes seen in Fgf8-deficient hypomorphic mice indicate that this protein has required functions at different times and locations during cardiogenesis and the subsequent OFT remodeling. Severe hypomorphs

have looping defects, reflecting a role for Fgf8 in embryonic and/or thoracic left-right axis determination (Meyers and Martin, 1999). Milder hypomorphs have hypoplastic OFTs and defects reflecting disrupted ventriculoarterial alignment (double outlet right ventricle, transposition of the great arteries) or failed OFT septation (persistent Truncus Arteriosus) (Abu-Issa et al., 2002; Frank et al., 2002).

The source(s) of Fgf8 required for outflow tract formation and subsequent remodeling are unknown. OFT development is normal after *Fgf8* loss-of-function in pharyngeal ectoderm (Macatee et al., 2003). Early widespread *Fgf8* ablation recapitulates the entire spectrum of OFT defects observed in hypomorphs (Brown et al., 2004), whereas later ablation throughout the caudal pharynx causes only a low incidence of an alignment-type OFT defect (Macatee et al., 2003) (A.M.M., unpublished).

In the wake of these studies, several important questions remain. Does the *Fgf8* expression domain in the cardiac crescent include both PHF and AHF cells, and what are the cellular targets of Fgf8 signaling in the crescent? What are the source(s) and timing of Fgf8 signals required for OFT formation and for Fgf8-dependent morphogenetic events during subsequent OFT remodeling? Is the source of Fgf8 required for OFT septation separable from that supporting rotation/alignment?

In order to address these questions, we determined the onset and breadth of *Fgf8* expression in the cardiac crescent, heart tube and pharynx. By precisely characterizing the activity of a series of Cre drivers relative to these *Fgf8* expression domains, we were able to examine and interpret the effects of *Fgf8* loss-of-function at specific times, and in particular cell populations, during the earliest stages of cardiogenesis and subsequent OFT remodeling. We found that autocrine Fgf8 signaling is required at the crescent stage to support formation of the heart tube and the RV/OFT, and for looping. Unlike the variable, complex phenotypes of previously reported *Fgf8* mutants, our approach generated discrete OFT defects in the face of normal embryonic LR axis specification and revealed specific, required roles for endoderm and mesoderm-derived Fgf8 in different aspects of OFT remodeling.

MATERIALS AND METHODS

Mice

Fgf8^{-}, *Fgf8*^{GFP}, *MesP1Cre*, *Mef2c-AHFCre* and *Tbx1*$^{-}$ alleles have been described previously (Jerome and Papaioannou, 2001; Macatee et al., 2003; Moon and Capecchi, 2000; Saga et al., 1999; Verzi et al., 2005). A novel *Fgf8*^{C} conditional allele was generated by inserting a loxP site 5′ to exon 4, and frt-flanked *neomycin*^{r} and a loxP site into the 3′ untranslated region. Construction of *Isl1*^{Cre} will be detailed elsewhere (C.-L.C. and S.E., unpublished); *Cre* was inserted in frame into exon 1 of *Isl1*, creating a *Cre* knock-in, *Isl1* knockout.

Immunohistochemistry and TUNEL analysis

Primary and secondary antibodies, and immunohistochemical methods have been previously described (Macatee et al., 2003). Anti-Isl1 antibody was described previously (Pfaff et al., 1996). Experiments were repeated a minimum of three times per somite stage.

Rosa26 Cre reporter lineage analysis

Embryos were stained for β-galactosidase activity resulting from Cre recombination of the Rosa26lacZ reporter (Soriano, 1999) using standard protocols; counterstaining was with nuclear Fast Red.

Whole mount in situ RNA hybridization

Embryos were harvested, fixed and hybridized using a standard protocol (Moon et al., 2006). Mutants and controls were processed in the same vial throughout. Experiments were repeated a minimum of three times; representative results are shown.

RESULTS

Fgf8 is expressed broadly in crescent mesoderm

To precisely characterize the timing and location of *Fgf8* expression within crescent mesoderm and pharynx, we used the $Fgf8^{GFP}$ conditional reporter allele (Macatee et al., 2003) and a universally expressed Cre recombinase, $HPRT^{Cre}$(Tang et al., 2002). Production of Fgf8GFP in *Fgf8*-expressing cells requires Cremediated recombination of $Fgf8^{GFP}$ and Fgf8GFP faithfully recapitulates the expression of the endogenous *Fgf8* locus throughout embryogenesis (Boulet et al., 2004; Ladher et al., 2005; Macatee et al., 2003).

In $Fgf8^{GFP/+}$;$HPRT^{Cre/+}$ embryos, myocardial precursors migrating anterolaterally from the primitive streak initiate *Fgf8* expression as they accumulate in the cardiac crescent at late headfold (LHF) to 1-somite stage (ss) (Fig. 1A,B). It has been proposed that *Fgf8* expression is limited to the AHF (Buckingham et al., 2005; Kelly and Buckingham, 2002); however, many LV precursors in the ventral heart tube express Fgf8GFP (Fig. 1C-E). At 10ss, Fgf8GFP persists in splanchnic mesoderm (SM) and nascent RV/OFT, but not in the LV or inflow (Fig. 1F,G). Rapid loss of GFP in the LV and inflow (already waning by 6ss, not shown) indicates that the half-life of the Fgf8GFP fusion protein is <10 hours in these cells. In the pharyngeal epithelia, Fgf8GFP is detectable in pouch endoderm and surface ectoderm by 5ss (Fig. 1D,E).

Given the broad expression of *Fgf8* in the crescent and early pharynx, and the complex phenotypes of previously reported *Fgf8* mutants, we assembled a panel of Cre-expressing ‘drivers’ to systematically generate *Fgf8* loss-of-function in subsets of myocardial precursor mesoderm and early endoderm. A detailed comparison of the activity of these drivers relative to *Fgf8* expression is crucial to interpreting and understanding the consequences of differential ablation of *Fgf8*; as will become apparent, subtle differences in the timing and location of *Fgf8* function profoundly influence ultimate phenotype.

MesP1Cre ablates Fgf8 in myocardial precursors prior to crescent formation

We used $MesP1^{Cre}$(Saga et al., 1999) to ablate *Fgf8* in all cardiac precursor mesoderm, as evidenced by *lacZ* expression from the Rosa26-Cre reporter throughout the cardiac crescent of presomite embryos, in the unlooped HT, and in all myocardium of embryonic day (E) 10.5 hearts (Fig. 1H-K) (Saga et al., 2000; Saga et al., 1999). In $Fgf8^{GFP/+}$;$MesP1^{Cre/+}$ embryos, Fgf8GFP is broadly detected in the crescent at LHF (1ss; Fig. 1A1,B1), in dorsal and ventral cells of the 5ss heart tube (Fig. 1C1,D1), and in AHF-derived RV/OFT (Fig. 1F1,G1). Mesodermal Fgf8GFP expression resulting from HPRTCre and MesP1Cre activity is indistinguishable (compare Fig. 1A-G with 1A1-1G1), indicating that MesP1Cre completely ablates *Fgf8* in the precardiac mesoderm.

Isl1Cre ablates Fgf8 in a subset of myocardial precursors and in endoderm

Fgf8 is expressed in the pharyngeal endodermal pouches, but its role in this tissue is unknown. Because *Isl1* is expressed broadly in pharyngeal endoderm and throughout the AHF (Cai et al., 2003), we generated a new, highly efficient ‘Isl1Cre’-expressing line to determine whether the loss of endodermal Fgf8 contributes to the cardiac or OFT defects observed in previously described *Fgf8* mutants. Isl1Cre-mediated recombination of the Rosa26-lacZ reporter is first evident in pharyngeal endoderm and crescent mesoderm at the 1-2ss (Fig. 1L). Its activity

expands rapidly such that, by 5ss, the first pouch and adjacent endoderm, and many cells in the ventral heart tube, are *lacZ*-positive (Fig. 1M-O2).

Fgf8GFP is not reproducibly detected in the cardiac crescent of $Fgf8^{GFP/+}$;$Isl1^{Cre/+}$ embryos until 2-3ss (Fig. 1A2,B2). Notably, fewer GFP-positive cells are present in the ventral 5ss heart tube of $Fgf8^{GFP/+}$;$Isl1^{Cre/+}$(Fig. 1C2,D2) than in either $Fgf8^{GFP/+}$;$MesP1^{Cre/+}$ or $Fgf8^{GFP/+}$;$HPRT^{Cre/+}$ embryos, suggesting that the *Fgf8* expression domain is broader than that of Isl1 (and the AHF) at the crescent stage. At 5ss, Fgf8GFP is already present in pouch endoderm and in scattered ectodermal cells. Endodermal Fgf8GFP expression resulting from Isl1Cre and HPRTCre activity is comparable from 5ss forward, indicating that Isl1Cre ablates *Fgf8* throughout the *Fgf8* endodermal expression domains (compare Fig. 1D-G with 1D2-G2).

Mef2C-AHFCre ablates Fgf8 in the AHF at the 2- to 3-somite stage

To assess whether *Fgf8* is required independently in AHF mesoderm, we employed Mef2c-AHFCre. Consistent with published activity of this driver (Verzi et al., 2005), Fgf8GFP is present in few AHF cells of $Fgf8^{GFP/+}$;*Mef2c-AHFCre* embryos at 2-3ss, but throughout the AHF by 5ss (Fig. 1A3-E3). In contrast to MesP1Cre and Isl1Cre, no Fgf8GFP-positive cells were present in LV precursors in the ventral heart tube of 5ss $Fgf8^{GFP/+}$;*Mef2c-AHFCre* embryos (Fig. 1D3,R).

The later onset and restricted domains of recombination in cardiac mesodermal precursors of Mef2c-AHFCre and Isl1Cre relative to MesP1Cre are summarized in Fig. 1P-S: Fgf8GFP is present in few crescent cells of $Fgf8^{GFP/+}$;$Isl1^{Cre/+}$ or $Fgf8^{GFP/+}$;*Mef2c-AHFCre* embryos prior to 2-3ss, which represents at least six hours of ongoing mesodermal Fgf8 signaling in these mutants relative to MesP1Cre (Fig. 1A1,B1 compare with A2,B2 and A3,B3). By 5ss, all three drivers are active throughout the SM/AHF, but only Isl1Cre has endodermal activity (Fig. 1R,S).

To generate *Fgf8* conditional mutants in the absence of confounding hypomorphic effects, we used a new loxP-containing allele with minimal exogenous sequence (abbreviated $Fgf8^{C}$, see Materials and methods). $Fgf8^{C/C}$ and$Fgf8^{C/-}$ animals are phenotypically normal and are indistinguishable from $Fgf8^{C/+}$ littermates.

Because $MesP1^{Cre}$ and $Isl1^{Cre}$ are loss-of-function alleles, we looked for evidence of genetic interaction with *Fgf8*. $Fgf8^{C/+}$;$MesP1^{Cre/+}$ embryos were morphologically and molecularly indistinguishable from $Fgf8^{C/+}$ or $Fgf8^{C/-}$ littermates and were present at the expected Mendelian ratios (E8-E11.5: *n*=79, 105% of predicted; E18.5/newborn: *n*=30,107% of predicted; Fig. 2A-C,L). Nor did we detect evidence of a genetic interaction between *Fgf8* and *Isl1* in Fgf8$^{C/+}$;$Isl1^{Cre/+}$ embryos (Fig. 2F-H,N; E8-E11.5: *n*=68, 100% of predicted; E18.5/newborn: *n*=26, 100% of predicted).

Autocrine Fgf8 activity in the crescent mesoderm is required for heart tube and outflow tract formation

Early, complete ablation of *Fgf8* function in both heart fields in $Fgf8^{C/-}$;$MesP1^{Cre/+}$ conditional mutants (*Fgf8;MesP1Cre*) disrupted HT formation, looping, and accretion of OFT/RV myocardium. These severely affected embryos (66/103, 65%) had hypoplastic heart tubes (Fig. 2E), short or absent OFTs, and a single dilated ventricle and atrium (Fig. 2E′), and died by E10.0 with anasarca and pericardial effusion (Fig. 2M′). This phenotype is also seen after ablation of *Fgf8* with Nkx2.5Cre (E. Meyers, unpublished). The lower incidence of this severe phenotype in $Fgf8^{C/-}$;$Isl1^{Cre/+}$ mutants (26/73, 35%; Fig. 2J,J′,O′) correlates with a later onset and a restricted domain of Isl1Cre activity in crescent mesoderm. By contrast, AHF-limited *Fgf8* ablation driven by Mef2c-AHFCre permitted all *Fgf8;Mef2c-AHFCre* mutants to survive

to birth (*n*=16, 105% of expected) after normal initial formation of the heart tube, OFT and RV (Fig. 2K,K′,P′).

Fgf8 in AHF mesoderm supports normal outflow tract alignment

Differences in Fgf8 signaling obtained after MesP1Cre, Isl1Cre and Mef2c-AHFCre ablation were not only manifest in the frequency of cardiac hypoplasia and embryonic death, but also in the OFT remodeling phenotypes of surviving mutants. Thirty-five percent of *Fgf8;MesP1Cre* mutants survived but had short, narrow OFTs and small RVs at midgestation (Fig. 2D,D′,M). Based on their embryonic phenotypes, we expected these mild mutants to have hypoplastic RVs at birth, but they did not; rather, 30% had D-transposition of the great arteries (TGA, *n*=15; Fig. 2R). This indicates that OFT rotation/alignment was perturbed by the loss of mesodermal Fgf8 and the resulting deficiency of RV/OFT myocardium at the time of OFT remodeling. Intrathoracic and intrabdominal LR axes appeared to be normal. Forty percent of *Fgf8;MesP1Cre* newborns also had a bicuspid aortic or pulmonary valve (the LV-associated valve; Fig. 2R′). No OFT or valve defects were observed in $Fgf8^{C/-}$ or $Fgf8^{C/+}$;$MesP1^{Cre/+}$ controls (*n*=28). The importance of post-crescent stage mesodermal Fgf8 for subsequent OFT alignment was confirmed by the occurrence of TGA and double outlet right ventricle (DORV) in $Fgf8^{C/-}$;*Mef2c-AHFCre* mutants (25%, *n*=16; Fig. 2S,S′). These findings allow us to attribute the OFT rotation/alignment and valve defects previously described in *Fgf8* hypomorphs, *Fgf8;Hoxa3IresCre* mutants and *Fgf8;Tbx1Cre* mutants (Abu-Issa et al., 2002; Frank et al., 2002; Macatee et al., 2003; Brown et al., 2004) specifically to disrupted autocrine Fgf8 function in AHF mesoderm.

Outflow tract septation requires Fgf8 function in the pharyngeal endoderm

Rather than alignment-type OFT defects, some *Fgf8* hypomorphs have persistent Truncus Arteriosus (PTA), in which failed OFT septation leaves a single vessel arising from both ventricles (Abu-Issa et al., 2002; Frank et al., 2002). Septated OFTs in all surviving *Fgf8;MesP1Cre* and *Fgf8;Mef2c-AHFCre* mesodermal mutants, and after ablation of Fgf8 from pharyngeal ectoderm (Macatee et al., 2003), indicates that septation is independent of these sources and is likely to depend on endodermal Fgf8.

Most $Fgf8^{C/-}$;$Isl1^{Cre/+}$ mutants survived embryogenesis (E18.5/newborn: *n*=18, 65% of predicted). At E8.75-E10.5 they had small pharyngeal arches and severe RV hypoplasia, with a markedly altered relationship between the LV and OFT (Fig. 2I,I′,O). $Fgf8^{C/-}$;$Isl1^{Cre/+}$ conotruncal cushions were hypocellular relative to controls; fusion of the conotruncal cushions to form the AP septum was already underway in E10.5 $Fgf8^{C/+}$;$Isl1^{Cre/+}$ controls, but not in $Fgf8^{C/-}$;$Isl1^{Cre/+}$ mutants (Fig. 2N,O). Remarkably, 100% of E18.5/newborn *Fgf8;Isl1Cre* mutants had PTA. The truncal vessel was abnormally positioned over the RV (Fig. 2T-T″), which is surprising given the severity of RV hypoplasia observed at midgestation.

Loss of Fgf8 in crescent mesoderm disrupts Erm and Isl1 expression in the AHF, and alters the balance between proliferation and cell death in the nascent heart

In order to understand the etiology of the early shared phenotype of MesP1Cre and Isl1Cre mutants, namely the disrupted formation of primary heart tube and OFT/RV, we sought to identify Fgf8-sensitive tissues at crescent and early somite stages and thus examined the expression of *Erm*. *Erm* is regulated by Fgf8 and encodes an Ets-domain transcription factor that is an effector of Fgf/Fgf receptor signaling (Brent and Tabin, 2004; Firnberg and Neubuser, 2002; Raible and Brand, 2001). In severe *Fgf8;MesP1Cre* and *Fgf8;Isl1Cre* mutants, decreased size and lower intensity of the *Erm* expression domain are apparent relative to controls and to mildly affected *Fgf8;MesP1Cre* mutants (Fig. 3A-F). *Erm* was absent in proximal OFT myocardium, and decreased in SM of both classes of mutants (Fig. 3A′-F′). Endodermal

Erm expression was more severely decreased in *Fgf8;Isl1Cre* mutants, suggesting autocrine Fgf8 activity in the endoderm (Fig. 3F′).

Isl1 is a LIM-homeodomain transcription factor required for the survival and proliferation of AHF mesoderm (Cai et al., 2003). We examined *Isl1* expression by in situ hybridization and Isl1 protein production with an anti-Isl1 antibody (Pfaff et al., 1996). Early disruption of *Isl1* expression in *Fgf8;MesP1Cre* and *Fgf8;Isl1Cre* mutants mirrored those observed in *Erm* (Fig. 3G-L). This is not attributable to the *Isl1* loss-of-function allele in $Fgf8^{C/-};Isl1^{Cre/+}$ mutants because Isl1 mRNA and protein production are decreased in MesP1Cre mutants (Fig. 3I), and are more severe in $Fgf8^{C/-};Isl1^{Cre/+}$ mutants than in $Fgf8^{C/+};Isl1^{Cre/+}$ controls (Fig. 3L,K). Analysis of Isl1 protein revealed both fewer Isl1-producing cells in SM, and less intense Isl1 immunostaining in cells in SM, proximal OFT and endoderm of conditional mutants relative to controls (Fig. 3M-P″). Levels of *Isl1* mRNA correlated with the severity of OFT defects observed in E9.5 MesP1Cre or Isl1Cre mutants: embryos dying with severe OFT/RV hypoplasia and incomplete looping had a markedly decreased intensity of *Isl1* expression in SM and endoderm (Fig. 3Q-V′).

We investigated whether the survival or expansion of cardiac precursors was decreased by a loss of Fgf8 in the crescent mesoderm and reasoned that PHF/AHF dysfunction must occur early in cardiogenesis in mutants, because abnormal heart tube and OFT morphology, and decreased Isl1 immunostaining were evident at 7-9ss. No reproducible increase in apoptosis was observed in mutant mesoderm at 0-4ss (Fig. 4A-F; data not shown), although apoptosis in neuroectoderm and ventral endoderm of mutants was increased relative to controls after 0ss (Fig. 4C-F). At 7-9ss, we detected excess apoptotic cells in ventral endoderm and adjacent midline SM accumulating to the OFT in both MesP1Cre and Isl1Cre mutants (Fig. 3M-P′, Fig. 4E-J), relative to double heterozygote controls (P=0.004, paired t-test; controls mean=9 cells/high-power field, n=6; mutants mean=22 cells/high-power field, n=4 *Fgf8;MesP1Cre* and n=5 *Fgf8;Isl1Cre* mutants).

Anti-PHH3 labels cells in all phases of mitosis (Li et al., 2005). At 0ss, high levels of proliferation were detected in both mutants and controls; notably the mutants had more PHH3-positive cells in the neuroectoderm, but fewer in the mesoderm and endoderm than controls (Fig. 4A,B). 4ss mutants had an average of 46% fewer proliferating cells in crescent mesoderm (Fig. 4E,F; P=0.005, paired t-test; controls mean=66%, n=4; *Fgf8;MesP1Cre* mutants mean=20%, n=4) and this difference persisted at 9ss. Fewer PHH3-positive cells were also noted in the proximal OFT and pharyngeal epithelia of 9ss conditional mutants (Fig. 4G-J).

Ablation of Fgf8 in mesoderm disrupts required transcription factor and signaling pathways in the anterior heart field and outflow tract without perturbing the left/right axis

To characterize the molecular events associated with disrupted growth of the OFT/RV in *Fgf8;MesP1Cre* and *Fgf8;Isl1Cre* conditional mutants, we examined gene expression in the AHF/nascent OFT. Expression of *Mef2c* is regulated by Isl1 and Foxh1 via AHF-specific enhancers (Dodou et al., 2004; von Both et al., 2004). When RV/OFT-fated myocardium first accrues to the heart (7-8ss in this system), expression of *Mef2c* in the AHF localizes to the right SM and nascent RV/OFT myocardium. This localization occurred in conditional mutants, but the level of *Mef2c* mRNA in OFT and SM was markedly decreased, whereas expression in the first pharyngeal arch and inflow was intact (Fig. 5A,A′). We attribute this alteration in *Mef2c* expression to the demonstrated decrease in Isl1 activity, because *Foxh1* expression was intact in *Fgf8;MesP1Cre* and *Fgf8;Isl1Cre* mutants (not shown).

Wnt11 influences cell adhesion, migration and polarity (McEwen and Peifer, 2000); it is expressed in truncal myocardium (Cai et al., 2003) and is required for OFT alignment and septation in mice (W. Zhou, L. Lin, A. Majumdar, X. Li, X. Zhang, W. Liu, L. Etheridge, Y.

Shi, J. Martin, W. Van de Ven, V. Kaartinen, A. Wynshaw-Boris, A. McMahon, M. G. Rosenfeld and S.E., unpublished). *Wnt11* expression correlated with the severity of RV/OFT dysplasia: it was undetectable in severe *Fgf8;MesP1Cre* and *Fgf8;Isl1Cre* mutants, decreased in mild variants, and preserved in *Fgf8;Mef2c-AHFCre* mutants (Fig. 5B,B′).

Disrupted heart looping is a feature of embryonic left-right (LR) axis disruption and it has been proposed that TGA and PTA may be manifestations of globally disrupted LR asymmetry (Bamforth et al., 2004). Fgf8 functions upstream of nodal and Pitx2c in embryonic LR axis determination (Boettger et al., 1999; Fischer et al., 2002; Kioussi et al., 2002; Liu et al., 2002; Meyers and Martin, 1999; Schneider et al., 1999; Welsh and O'Brien, 2000). We examined *Pitx2* expression to assess whether the looping and OFT defects observed in MesP1Cre and Isl1Cre *Fgf8* conditional mutants reflect the altered specification/maintenance of the embryonic LR axis and found that *Pitx2* localized appropriately to the left SM, OFT and atrial myocardium in mild and severely affected mutants at the 10-16ss (Fig. 5C-C″; data not shown). Normal expression of *Ventricular myosin light chain 2* (Franco et al., 1999) indicated that myocardial differentiation occurred in the hypoplastic right ventricles of conditional mutants (not shown).

Tbx1 is upstream of Fgf signaling in the pharyngeal endoderm

Tbx1 is required for OFT septation, as well as for cell proliferation and *Fgf10* expression in the AHF (Arnold et al., 2006; Xu et al., 2004). As *Tbx1* and *Fgf10* expression were intact in *Fgf8;MesP1Cre* and *Fgf8;Isl1Cre* mutants (Fig. 5D,E), disruption of these factors does not cause the observed OFT defects.

Based on the shared phenotypes of Fgf receptor 1 (*Fgfr1*) and *Fgf8* mutants, on recent data indicating that Fgfr1 is activated by Fgf8 in vivo (Moon et al., 2006), and on our unpublished observation that OFT septation is sensitive to Fgfr1 function, Fgfr1 probably mediates Fgf8 signals in target cells required for OFT septation. Moreover, decreased *Erm* expression in the endoderm of *Fgf8;Isl1Cre* mutants, which develop PTA, suggests that Fgf8 has an autocrine role in the endoderm required for OFT septation. It has previously been demonstrated that *Fgf8* expression is markedly decreased in the endoderm of $Tbx1^{-/-}$ mutants, in which PTA is attributable to loss of Tbx1 in the endoderm (Xu et al., 2004); thus, we questioned whether loss of *Tbx1* also disrupts *Fgfr1* expression and found a dosage-sensitive decrease in the expression of *Fgfr1* in the endoderm and mesenchyme, specifically in the caudal pharyngeal arches of *Tbx1* heterozygotes and null mutants (Fig. 6).

DISCUSSION

Our studies indicate that Fgf8 signaling to mesodermal myocardial precursors is required at presomite stages for the normal expression of *Isl1* and *Mef2c*, and for the proliferation of myocardial precursors during formation of the primary heart tube, RV and OFT. Our results also demonstrate that the sources and targets of Fgf8 required for OFT septation and rotation/alignment are not only temporally distinct from those for heart tube and OFT formation, but are spatially separate from one another (Fig. 7).

Autocrine Fgf8 signals in cardiac crescent mesoderm regulate heart tube and OFT formation, and the Isl1/Mef2c pathway in the AHF

Although no markers exist for the PHF, greater numbers of Fgf8GFP-positive LV precursors in the ventral heart tubes of $Fgf8^{GFP/+}$;$MesP1^{Cre/+}$ and $Fgf8^{GFP/+}$;$HPRT^{Cre/+}$ embryos than $Fgf8^{GFP/+}$;$Isl1^{Cre/+}$ embryos strongly suggest that *Fgf8* is expressed in both the PHF and the AHF. MesP1Cre reliably ablates early *Fgf8* function throughout the cardiac crescent, generating a high percentage of mutants with severe heart tube and RV/OFT hypoplasia (Fig.

7B). Although a small subset of *Fgf8;Isl1Cre* mutants display this severe phenotype, AHF-restricted mesodermal mutants (*Fgf8;Mef2c-AHFCre*) do not. The differences in timing and domain of these Cre drivers thus reveal a previously unknown role for autocrine Fgf8 signaling in the crescent mesoderm to support normal formation of the heart tube and AHF-derived tissues. Although we attribute the death of severe mutants to cardiac insufficiency from a decreased pump size and OFT obstruction, abnormal Fgf8 signaling may also disrupt myocardial calcium handling and cardiac function (Farrell et al., 2001).

Loss of *Fgf8* in the AHF/SM resulted in decreased *Erm* expression within the SM itself, providing additional evidence for autocrine Fgf8 activity in the AHF. Furthermore, we detected altered apoptosis/proliferation and decreased numbers of *Isl1*- and *Mef2c*-expressing cells in the AHF of mutants, suggesting that Fgf8 maintains the Isl1/Mef2c transcriptional cascade required for normal survival and accrual of AHF-derived cells to the heart. As *Wnt11* expression is undetectable in the OFT myocardium of severe *MesP1Cre* and *Isl1Cre* mutants (and in *Fgf8;Nkx2.5Cre* conditional mutants) (Ilagan et al., 2006), but is preserved in *Fgf8;Mef2cAHFCre* mutants, we conclude that *Wnt11* expression in AHF-derived myocardium depends on autocrine Fgf8 function in the AHF prior to the 2-3 ss.

It is unlikely that the survival of some *Fgf8;MesP1Cre* mutants is due to incomplete MesP1Cre recombination because, in our experience, and in work reported previously (Saga et al., 1999), this driver is active in all anterior primitive streak-derived mesoderm. Thus, we interpret the survival of some *Fgf8;MesP1Cre* mutants to indicate that other factor(s) can support heart tube and RV/OFT formation. Fgf10 is a candidate for functional redundancy, as its expression was intact in the mesoderm of these mutants. Experiments testing Fgf8/Fgf10 functional redundancy are underway.

Outflow tract alignment and septation are regulated by different Fgf8 tissue sources

The distinct OFT phenotypes of *MesP1Cre*, *Isl1Cre* and *Mef2c-AHFCre* mutants also reveal domain-specific functions of Fgf8 during OFT remodeling. TGA and DORV, observed in *Fgf8;MesP1Cre* and *Fgf8;Mef2c-AHFCre* mesoderm-only mutants, (Fig. 7D), exist along a spectrum of OFT alignment/rotation defects in which the Truncus is septated, but the great vessels are not aligned correctly with the ventricles. Conotruncal septal spiraling, conal involution and positioning, and OFT rotation (Lamers and Moorman, 2002) may be affected directly by loss of Fgf8 signaling, or indirectly by an insufficient quantity of OFT myocardium (Yelbuz et al., 2002).

In contrast to TGA/DORV, PTA (observed in 100% of *Fgf8;Isl1Cre* mutants, Fig. 7E) reflects a complete failure of OFT septation. Because PTA was observed in *Fgf8* hypomorphs and *Fgf8;Tbx1Cre* mutants (both of which have intact *Isl1* loci), it is unlikely that the failed septation in *Fgf8;Isl1Cre* mutants is due to the additive effects of *Fgf8* loss-of-function and *Isl1* heterozygosity. Furthermore, $Isl1^{Cre/+}$ and $Fgf8^{C/+};Isl1^{Cre/+}$ OFTs are normal. However, formal assessment of the contribution of *Isl1* haploinsufficiency to OFT defects observed in *Fgf8;Isl1Cre* mutants requires a Cre-expressor that ablates *Fgf8* in the same temporospatial domains as Isl1Cre.

Notably, in most human and mouse examples of PTA, the Truncus is normally aligned, straddling both ventricles (Bartelings and Gittenberger-de Groot, 1989; Xu et al., 2004; Yelbuz et al., 2002). However in *Fgf8;Isl1Cre* mutants (and $Tbx1^{-/-}$) (Xu et al., 2004; Zhang et al., 2005) the Truncus is abnormally aligned, 100% committed to the RV, indicating that the mechanism(s) that disrupt the alignment/rotation after loss of mesodermal Fgf8 in *Fgf8;MesP1Cre* mutants also operate in *Fgf8;Isl1Cre* endodermal/mesodermal mutants.

Cellular targets of Fgf8

Our conclusion that the endoderm mediates crucial Fgf8 signals to regulate OFT septation is consistent with studies indicating that PTA in Tbx1$^{-/-}$ mutants results from a loss of endodermal *Tbx1*, accompanied by a loss of *Fgf8* in this tissue (Arnold et al., 2006; Xu et al., 2004). Our finding of decreased *Fgfr1* expression in the endoderm of *Tbx1*$^{-/-}$ mutants indicates that Tbx1 function influences Fgf signaling at multiple levels, and provides new evidence that such crosstalk regulates OFT septation.

The OFT septum is formed by contributions from the endothelium (by epithelial to mesenchymal transformation) and the cardiac neural crest (CNC), so these are potential paracrine targets of endodermal Fgf8 (Fig. 7D,E). However, ablation of *Fgfr1* and/or *Fgfr2* in premigratory CNC does not cause OFT septation defects, so CNC is not a direct target of endodermal Fgf8 (L. Francis and A.M.M., unpublished) (Ilagan et al., 2006). By contrast, the ablation of *Fgfr1* and one copy of *Fgfr2* with Isl1Cre generates PTA at high penetrance (L. Francis, S.E. and A.M.M., unpublished). Because the Isl1Cre expression domain includes the mesodermal precursors of OFT endothelium (Fig. 1O1 and data not shown) and endoderm, further tissue-restricted receptor ablation analyses are required to determine whether PTA in *Fgf8* and Fgfr mutants results from disrupting paracrine and/or autocrine endodermal Fgf8 signaling.

When considered in the context of earlier studies, these findings provide new insight into the requisite timing of Fgf8 signals in different expression domains. Ablation of *Fgf8* with Nkx2.5Cre (Ilagan et al., 2006), or in precardiac mesoderm at E7.75-E8.0 (LHF-1ss), disrupts PHF and AHF function, causing severe phenotypes in *Fgf8;MesP1Cre* and some *Fgf8;Isl1Cre* mutants. Later ablation of *Fgf8* with a *Tbx1Cre* transgene (expressed in multiple domains from E8.5) generated both septation and alignment-type OFT defects (Brown et al., 2004). By contrast, only a low incidence of alignment-type defects occurred with *Fgf8* ablation after E9.0 using Hoxa3IresCre (Macatee et al., 2003). Thus, Fgf8 signals at E7.75-E8.0 in precardiac mesoderm are required for normal PHF and AHF function, whereas signaling from pharyngeal endoderm and splanchnic mesoderm, required for OFT septation and alignment/rotation, respectively, occurs prior to E9.0. This is an important finding, as invasion of the AP septum and OFT cushion fusion begin at least one day later (Lamers and Moorman, 2002).

Fgf8-related cardiovascular malformations and the embryonic left-right axis

Pitx2 mutants revealed that local, organ-specific LR axes can be determined independently of the embryonic LR axis and at different morphogenetic stages (Kioussi et al., 2002; Kitamura et al., 1999; Liu et al., 2001; Liu et al., 2002). It has been unclear whether looping defects and pulmonary isomerism of severe *Fgf8* hypomorphs (Meyers and Martin, 1999) reflect embryonic LR-axis disruption due to Fgf8 deficiency in the primitive streak or node, or later dysfunction in the SM that perturbs the intrathoracic LR axis. Preserved *Pitx2* lateralization in early stage *Fgf8;MesP1Cre* and *Fgf8;Isl1Cre* mutants (including those with altered looping) supports the former hypothesis. It remains to be determined whether disruption of a later, cardiac-specific LR pathway contributes to OFT remodeling defects in these conditional mutants.

Conclusion

The survival/proliferation and molecular analyses presented here focused on heart tube formation and the accumulation of RV/OFT myocardium in the absence of mesodermal Fgf8. Further studies are underway to examine these processes during OFT remodeling and to determine the bases of the distinct OFT defects observed in mesodermal versus endodermal *Fgf8* mutants. The primitive cardiovascular system must support the entire organism while

crucial aspects of its development are still underway and vulnerable to a variety of genetic or environmental insults. Genetic systems that reliably create specific cardiovascular defects are an important step towards ultimately dissecting how structural and hemodynamic inputs interact with, and modify, the genetic and molecular programs that control cardiac morphogenesis in normal and pathological conditions.

Acknowledgements

We thank Yumiko Saga and Virginia Papaioannou for kindly providing *MesP1Cre* and *Tbx1*¯ alleles, respectively, Charles Murtaugh for the generous gift of Isl1 antibody, and Jim Martin for the Pitx2 riboprobe. We thank Erik Meyers for discussing unpublished results. We are grateful to Kirk Thomas, Chris Lehman, James Martin and Yukio Saijoh for critically reading the manuscript and suggestions. Tim Macatee and Jaclyn Tygesen provided technical assistance. This work was supported by grants from NIH/CHHD (R01HD044157, A.M.M.) and the AHA (A.M.M.), and from the University of Utah Children's Health Research Center (D.U.F.).

References

Abu-Issa R, Smyth G, Smoak I, Yamamura KI, Meyers EN. Fgf8 is required for pharyngeal arch and cardiovascular development in the mouse. Development 2002;129:4613–4625. [PubMed: 12223417]

Armstrong EJ, Bischoff J. Heart valve development: endothelial cell signaling and differentiation. Circ. Res 2004;95:459–470. [PubMed: 15345668]

Arnold JS, Werling U, Braunstein EM, Liao J, Nowotschin S, Edelmann W, Hebert JM, Morrow BE. Inactivation of Tbx1 in the pharyngeal endoderm results in 22q11DS malformations. Development 2006;133:977–987. [PubMed: 16452092]

Bamforth SD, Braganca J, Farthing CR, Schneider JE, Broadbent C, Michell AC, Clarke K, Neubauer S, Norris D, Brown NA, et al. Cited2 controls left-right patterning and heart development through a Nodal-Pitx2c pathway. Nat. Genet 2004;36:1189–1196. [PubMed: 15475956]

Bartelings MM, Gittenberger-de Groot AC. The outflow tract of the heart-embryologic and morphologic correlations. Int. J. Cardiol 1989;22:289–300. [PubMed: 2651326]

Boettger T, Wittler L, Kessel M. FGF8 functions in the specification of the right body side of the chick. Curr. Biol 1999;9:277–280. [PubMed: 10074453]

Boulet AM, Moon AM, Arenkiel BR, Capecchi MR. The roles of Fgf4 and Fgf8 in limb bud initiation and outgrowth. Dev. Biol 2004;273:361–372. [PubMed: 15328019]

Brand T. Heart development: molecular insights into cardiac specification and early morphogenesis. Dev. Biol 2003;258:1–19. [PubMed: 12781678]

Brent AE, Tabin CJ. FGF acts directly on the somitic tendon progenitors through the Ets transcription factors Pea3 and Erm to regulate scleraxis expression. Development 2004;131:3885–3896. [PubMed: 15253939]

Brown CB, Wenning JM, Lu MM, Epstein DJ, Meyers EN, Epstein JA. Cre-mediated excision of Fgf8 in the Tbx1 expression domain reveals a critical role for Fgf8 in cardiovascular development in the mouse. Dev. Biol 2004;267:190–202. [PubMed: 14975726]

Bruneau BG. Transcriptional regulation of vertebrate cardiac morphogenesis. Circ. Res 2002;90:509–519. [PubMed: 11909814]

Buckingham M, Meilhac S, Zaffran S. Building the mammalian heart from two sources of myocardial cells. Nat. Rev. Genet 2005;6:826–835. [PubMed: 16304598]

Cai CL, Liang X, Shi Y, Chu PH, Pfaff SL, Chen J, Evans S. Isl1 identifies a cardiac progenitor population that proliferates prior to differentiation and contributes a majority of cells to the heart. Dev. Cell 2003;5:877–889. [PubMed: 14667410]

Creazzo TL, Godt RE, Leatherbury L, Conway SJ, Kirby ML. Role of cardiac neural crest cells in cardiovascular development. Annu. Rev. Physiol 1998;60:267–286. [PubMed: 9558464]

Cripps RM, Olson EN. Control of cardiac development by an evolutionarily conserved transcriptional network. Dev. Biol 2002;246:14–28. [PubMed: 12027431]

Crossley PH, Martin GR. The mouse Fgf8 gene encodes a family of polypeptides and is expressed in regions that direct outgrowth and patterning in the developing embryo. Development 1995;121:439–451. [PubMed: 7768185]

de la Cruz MV, Sanchez Gomez C, Arteaga MM, Arguello C. Experiental study of the development of the truncus and the conus in the chick embryo. J. Anat 1977;123:661–686. [PubMed: 885781]

de la Cruz MV, Markwald RR, Krug EL, Rumenoff L, Sanchez Gomez C, Sadowinski S, Galicia TD, Gomez F, Salazar Garcia M, Villavicencio Guzman L, et al. Living morphogenesis of the ventricles and congenital pathology of their component parts. Cardiol. Young 2001;11:588–600. [PubMed: 11813909]

Delot EC, Bahamonde ME, Zhao M, Lyons KM. BMP signaling is required for septation of the outflow tract of the mammalian heart. Development 2003;130:209–220. [PubMed: 12441304]

Dodou E, Verzi MP, Anderson JP, Xu SM, Black BL. Mef2c is a direct transcriptional target of ISL1 and GATA factors in the anterior heart field during mouse embryonic development. Development 2004;131:3931–3942. [PubMed: 15253934]

Farrell MJ, Burch JL, Wallis K, Rowley L, Kumiski D, Stadt H, Godt RE, Creazzo TL, Kirby ML. FGF-8 in the ventral pharynx alters development of myocardial calcium transients after neural crest ablation. J. Clin. Invest 2001;107:1509–1517. [PubMed: 11413158]

Firnberg N, Neubuser A. FGF signaling regulates expression ofTbx2, Erm, Pea3, and Pax3 in the early nasal region. Dev. Biol 2002;247:237–250. [PubMed: 12086464]

Firulli AB, Thattaliyath BD. Transcription factors in cardiogenesis: the combinations that unlock the mysteries of the heart. Int. Rev. Cytol 2002;214:1–62. [PubMed: 11893163]

Fischer A, Viebahn C, Blum M. FGF8 acts as a right determinant during establishment of the left-right axis in the rabbit. Curr. Biol 2002;12:1807–1816. [PubMed: 12419180]

Fishman MC, Chien KR. Fashioning the vertebrate heart: earliest embryonic decisions. Development 1997;124:2099–2117. [PubMed: 9187138]

Franco D, Markman MM, Wagenaar GT, Ya J, Lamers WH, Moorman AF. Myosin light chain 2a and 2v identifies the embryonic outflow tract myocardium in the developing rodent heart. Anat. Rec 1999;254:135–146. [PubMed: 9892427]

Frank DU, Fotheringham LK, Brewer JA, Muglia LJ, Tristani Firouzi M, Capecchi MR, Moon AM. An Fgf8 mouse mutant phenocopies human 22q11 deletion syndrome. Development 2002;129:4591–4603. [PubMed: 12223415]

Harvey RP. Patterning the vertebrate heart. Nat. Rev. Genet 2002;3:544–556. [PubMed: 12094232]

Ilagan R, Abu-Issa R, Brown D, Yang Y, Jiao K, Schwartz R, Klingensmith J, Meyers EN. *Fgf8* is required for anterior heart field development. Development 2006:2435–2445. [PubMed: 16720880]

Jerome LA, Papaioannou VE. DiGeorge syndrome phenotype in mice mutant for the T-box gene, Tbx1. Nat. Genet 2001;27:286–291. [PubMed: 11242110]

Kelly RG, Buckingham ME. The anterior heart-forming field: voyage to the arterial pole of the heart. Trends Genet 2002;18:210–216. [PubMed: 11932022]

Kelly RG, Brown NA, Buckingham ME. The arterial pole of the mouse heart forms from Fgf10-expressing cells in pharyngeal mesoderm. Dev. Cell 2001;1:435–440. [PubMed: 11702954]

Kioussi C, Briata P, Baek SH, Wynshaw-Boris A, Rose DW, Rosenfeld MG. Pitx genes during cardiovascular development. Cold Spring Harb. Symp. Quant. Biol 2002;67:81–87. [PubMed: 12858527]

Kitamura K, Miura H, Miyagawa-Tomita S, Yanazawa M, Katoh-Fukui Y, Suzuki R, Ohuchi H, Suehiro A, Motegi Y, Nakahara Y, et al. Mouse Pitx2 deficiency leads to anomalies of the ventral body wall, heart, extra- and periocular mesoderm and right pulmonary isomerism. Development 1999;126:5749–5758. [PubMed: 10572050]

Ladher RK, Wright TJ, Moon AM, Mansour SL, Schoenwolf GC. FGF8 initiates inner ear induction in chick and mouse. Genes Dev 2005;19:603–613. [PubMed: 15741321]

Lamers WH, Moorman AF. Cardiac septation: a late contribution of the embryonic primary myocardium to heart morphogenesis. Circ. Res 2002;91:93–103. [PubMed: 12142341]

Li DW, Yang Q, Chen JT, Zhou H, Liu RM, Huang XT. Dynamic distribution of Ser-10 phosphorylated histone H3 in cytoplasm of MCF-7 and CHO cells during mitosis. Cell Res 2005;15:120–126. [PubMed: 15740641]

Lin Q, Schwarz J, Bucana C, Olson EN. Control of mouse cardiac morphogenesis and myogenesis by transcription factor MEF2C. Science 1997;276:1404–1407. [PubMed: 9162005]

Liu C, Liu W, Lu MF, Brown NA, Martin JF. Regulation of left-right asymmetry by thresholds of Pitx2c activity. Development 2001;128:2039–2048. [PubMed: 11493526]

Liu C, Liu W, Palie J, Lu MF, Brown NA, Martin JF. Pitx2c patterns anterior myocardium and aortic arch vessels and is required for local cell movement into atrioventricular cushions. Development 2002;129:5081–5091. [PubMed: 12397115]

Liu W, Selever J, Wang D, Lu MF, Moses KA, Schwartz RJ, Martin JF. Bmp4 signaling is required for outflow-tract septation and branchial-arch artery remodeling. Proc. Natl. Acad. Sci. USA 2004;101:4489–4494. [PubMed: 15070745]

Lough J, Sugi Y. Endoderm and heart development. Dev. Dyn 2000;217:327–342. [PubMed: 10767078]

Macatee TL, Hammond BP, Arenkiel BR, Francis L, Frank DU, Moon AM. Ablation of specific expression domains reveals discrete functions of ectoderm- and endoderm-derived FGF8 during cardiovascular and pharyngeal development. Development 2003;130:6361–6374. [PubMed: 14623825]

McEwen DG, Peifer M. Wnt signaling: Moving in a new direction. Curr. Biol 2000;10:R562–R564. [PubMed: 10959830]

Meyers EN, Martin GR. Differences in left-right axis pathways in mouse and chick: functions of FGF8 and SHH. Science 1999;285:403–406. [PubMed: 10411502]

Min H, Danilenko DM, Scully SA, Bolon B, Ring BD, Tarpley JE, DeRose M, Simonet WS. Fgf-10 is required for both limb and lung development and exhibits striking functional similarity to Drosophila branchless. Genes Dev 1998;12:3156–3161. [PubMed: 9784490]

Mjaatvedt CH, Nakaoka T, Moreno-Rodriguez R, Norris RA, Kern MJ, Eisenberg CA, Turner D, Markwald RR. The outflow tract of the heart is recruited from a novel heart-forming field. Dev. Biol 2001;238:97–109. [PubMed: 11783996]

Moon AM, Capecchi MR. FGF8 is required for outgrowth and patterning of the limbs. Nat. Genet 2000;26:455–459. [PubMed: 11101845]

Moon AM, Guris DL, Seo JH, Li L, Hammond J, Talbot A, Imamoto A. Crkl deficiency disrupts fgf8 signaling in a mouse model of 22q11 deletion syndromes. Dev. Cell 2006;10:71–80. [PubMed: 16399079]

Olson EN, Schneider MD. Sizing up the heart: development redux in disease. Genes Dev 2003;17:1937–1956. [PubMed: 12893779]

Pfaff SL, Mendelsohn M, Stewart CL, Edlund T, Jessell TM. Requirement for LIM homeobox gene Isl1 in motor neuron generation reveals a motor neuron-dependent step in interneuron differentiation. Cell 1996;84:309–320. [PubMed: 8565076]

Raible F, Brand M. Tight transcriptional control of the ETS domain factors Erm and Pea3 by Fgf signaling during early zebrafish development. Mech. Dev 2001;107:105–117. [PubMed: 11520667]

Saga Y, Miyagawa-Tomita S, Takagi A, Kitajima S, Miyazaki J, Inoue T. MesP1 is expressed in the heart precursor cells and required for the formation of a single heart tube. Development 1999;126:3437–3447. [PubMed: 10393122]

Saga Y, Kitajima S, Miyagawa-Tomita S. Mesp1 expression is the earliest sign of cardiovascular development. Trends Cardiovasc. Med 2000;10:345–352. [PubMed: 11369261]

Sanford LP, Ormsby I, Gittenberger-de Groot AC, Sariola H, Friedman R, Boivin GP, Cardell EL, Doetschman T. TGFbeta2 knockout mice have multiple developmental defects that are non-overlapping with other TGFbeta knockout phenotypes. Development 1997;124:2659–2670. [PubMed: 9217007]

Schneider A, Mijalski T, Schlange T, Dai W, Overbeek P, Arnold HH, Brand T. The homeobox gene NKX3.2 is a target of left-right signalling and is expressed on opposite sides in chick and mouse embryos. Curr. Biol 1999;9:911–914. [PubMed: 10469600]

Schultheiss TM, Xydas S, Lassar AB. Induction of avian cardiac myogenesis by anterior endoderm. Development 1995;121:4203–4214. [PubMed: 8575320]

Sekine K, Ohuchi H, Fujiwara M, Yamasaki M, Yoshizawa T, Sato T, Yagishita N, Matsui D, Koga Y, Itoh N, et al. Fgf10 is essential for limb and lung formation. Nat. Genet 1999;21:138–141. [PubMed: 9916808]

Soriano P. Generalized lacZ expression with the ROSA26 Cre reporter strain. Nat. Genet 1999;21:70–71. [PubMed: 9916792]

Srivastava D, Olson EN. A genetic blueprint for cardiac development. Nature 2000;407:221–226. [PubMed: 11001064]

Sun X, Meyers EN, Lewandoski M, Martin GR. Targeted disruption of Fgf8 causes failure of cell migration in the gastrulating mouse embryo. Genes Dev 1999;13:1834–1846. [PubMed: 10421635]

Tang SH, Silva FJ, Tsark WM, Mann JR. A Cre/loxP-deleter transgenic line in mouse strain 129S1/SvImJ. Genesis 2002;32:199–202. [PubMed: 11892008]

Verzi MP, McCulley DJ, De Val S, Dodou E, Black BL. The right ventricle, outflow tract, and ventricular septum comprise a restricted expression domain within the secondary/anterior heart field. Dev. Biol 2005;287:134–145. [PubMed: 16188249]

von Both I, Silvestri C, Erdemir T, Lickert H, Walls JR, Henkelman RM, Rossant J, Harvey RP, Attisano L, Wrana JL. Foxh1 is essential for development of the anterior heart field. Dev. Cell 2004;7:331–345. [PubMed: 15363409]

Waldo KL, Kumiski DH, Wallis KT, Stadt HA, Hutson MR, Platt DH, Kirby ML. Conotruncal myocardium arises from a secondary heart field. Development 2001;128:3179–3188. [PubMed: 11688566]

Welsh IC, O'Brien TP. Loss of late primitive streak mesoderm and interruption of left-right morphogenesis in the Ednrb(s-1Acrg) mutant mouse. Dev. Biol 2000;225:151–168. [PubMed: 10964471]

Xu H, Morishima M, Wylie JN, Schwartz RJ, Bruneau BG, Lindsay EA, Baldini A. Tbx1 has a dual role in the morphogenesis of the cardiac outflow tract. Development 2004;131:3217–3227. [PubMed: 15175244]

Yelbuz TM, Waldo KL, Kumiski DH, Stadt HA, Wolfe RR, Leatherbury L, Kirby ML. Shortened outflow tract leads to altered cardiac looping after neural crest ablation. Circulation 2002;106:504–510. [PubMed: 12135953]

Yutzey KE, Kirby ML. Wherefore heart thou? Embryonic origins of cardiogenic mesoderm. Dev. Dyn 2002;223:307–320. [PubMed: 11891982]

Zaffran S, Kelly RG, Meilhac SM, Buckingham ME, Brown NA. Right ventricular myocardium derives from the anterior heart field. Circ. Res 2004;95:261–268. [PubMed: 15217909]

Zhang Z, Cerrato F, Xu H, Vitelli F, Morishima M, Vincentz J, Furuta Y, Ma L, Martin JF, Baldini A, et al. Tbx1 expression in pharyngeal epithelia is necessary for pharyngeal arch artery development. Development 2005;132:5307–5315. [PubMed: 16284121]

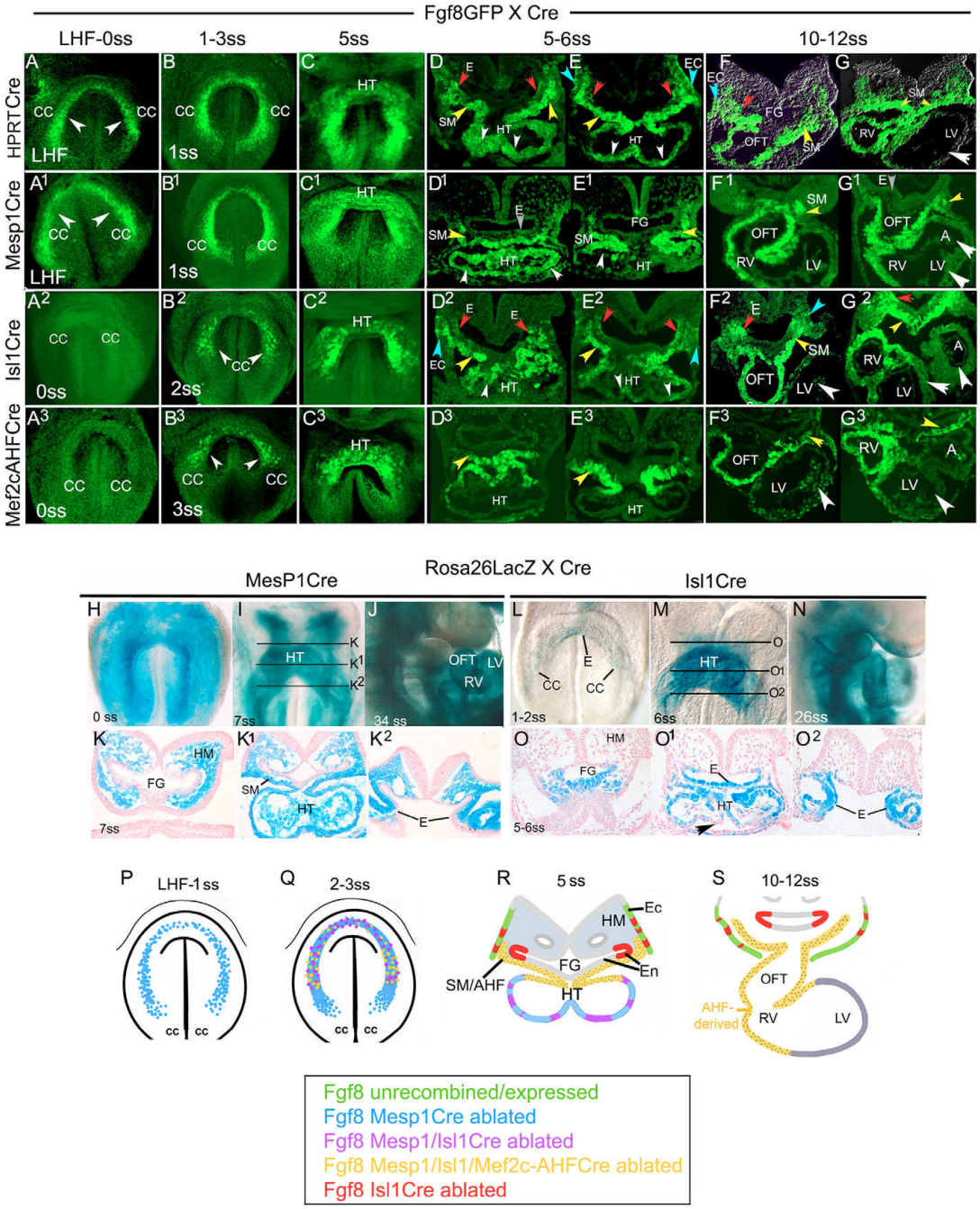

Fig. 1.

Differential activity of MesP1Cre, Isl1Cre and Mef2cAHFCre relative to Fgf8 expression domains in cardiac crescent and early pharynx. (**A-G**) Anti-GFP immunohistochemistry in $Fgf8^{GFP/+}$;$HPRT^{Cre/+}$ embryos reveals the onset and location of all *Fgf8* expression in the cardiac crescent and pharynx. (A-C) Whole-mount preparations show Fgf8GFP is already broadly expressed in the cardiac crescent (cc) by the LHF stage, and in the heart tube (HT) and AHF/SM at 5ss. (D,E) 6ss; transverse sections, anterior to posterior through the heart tube. Cells in the HT (white arrowheads), AHF/SM (yellow arrowheads), foregut (FG), first pouch endoderm (E, red arrowheads) and surface ectoderm (EC, blue arrowheads) are GFP positive. (F,G) 10ss (combined DIC/epifluorescence); Fgf8GFP is present in pharyngeal epithelia, SM

and RV/OFT (yellow arrowheads), but not in the left ventricle (LV, white arrowhead). (A1-G1) Fgf8GFP expression in *Fgf8*$^{GFP/+}$;*MesP1Cre*$^{/+}$ embryos. (A1-C1) Whole-mounts demonstrate Fgf8GFP broadly in the cardiac crescent at LHF and 1ss, and in the HT at 5ss. (D1,E1) 5ss transverse sections; Fgf8GFP is in the HT and SM; endoderm is GFP-negative (gray arrowhead). (F1,G1) 12ss transverse sections; the LV and atrium are now Fgf8GFP negative (white arrowheads). (A2-G2) Fgf8GFP expression in *Fgf8*$^{GFP/+}$;*Isl1*$^{Cre/+}$ embryos. (A2-C2) Isl1Cre is not active in the cardiac crescent at 0ss (A2), but Fgf8GFP is present at 2ss (B2) and is widely expressed at 5ss (C2). (D2,E2) Pouch endoderm, SM, and ventral HT cells in 5ss embryos are Fgf8GFP positive. (F2,G2) 11ss; transverse sections reveal Fgf8GFP in pharyngeal epithelia, SM and OFT/RV but not in the LV or atrium (A). (A3-G3) *Fgf8*$^{GFP/+}$;*Mef2cAHFCre* embryos. Mef2cAHFCre is not active at 0ss and little GFP is detected in AHF mesoderm until 3ss (B3). Note the lack of expression in any ventral HT cells (D3); expression is restricted to the AHF/SM (E3) and RV/OFT (F3). (H-O2) Comparison of MesP1Cre and Isl1Cre recombination using the Rosa26R-Cre reporter and β-galactosidase staining. (**H-J**) Whole mounts MesP1Cre-recombined at 0, 7ss (ventral views) and 34ss (right lateral). (**K-K2**) 7ss transverse sections of a MesP1Cre/Rosa26R embryo; recombination is evident throughout the head mesoderm (HM), SM and HT, and is restricted to mesoderm. (**L-N**) Whole mounts of Isl1Cre/Rosa26R embryos. At 1ss (L), few crescent cells are labeled. (M) 6ss, ventral view; black lines depict plane of sections shown in panels O-O2. (N) 24ss, right lateral view; pharyngeal arches and entire RV/OFT are labeled. (O-O2) 6ss transverse sectioned Isl1Cre/Rosa26R embryo; recombination is evident in the foregut (FG), endoderm (E), SM and many HT cells; scattered ventral myocardial cells that are unstained are indicated by the black arrowhead. Rare pharyngeal ectodermal (EC) cells are stained. (P-S) Schematics comparing the timing and location of *Fgf8* ablation by different Cre drivers. (**P**,**Q**) Whole mounts at LHF-1ss and 2-3ss; *Fgf8* is ablated in all myocardial precursors by MesP1Cre (blue); the onset of Isl1Cre is later and in fewer cells (purple); followed by Mef2c-AHFCre only in the AHF at the 3ss (yellow indicates that all three Cre drivers active). Note that the dorsoventral location of these populations is not depicted. (**R**) Transverse section at 5ss; Isl1Cre is active in pouch endoderm and surface ectoderm (red); all three drivers recombine the SM/AHF and dorsal HT. MesP1Cre ablates *Fgf8* in more ventral HT cells, suggesting that *Fgf8* is expressed in both heart fields. (**S**) Transverse section at 10-12ss; all three drivers ablate *Fgf8* in SM and AHF-derived RV/OFT (yellow); *Fgf8* is no longer expressed in the LV (gray).

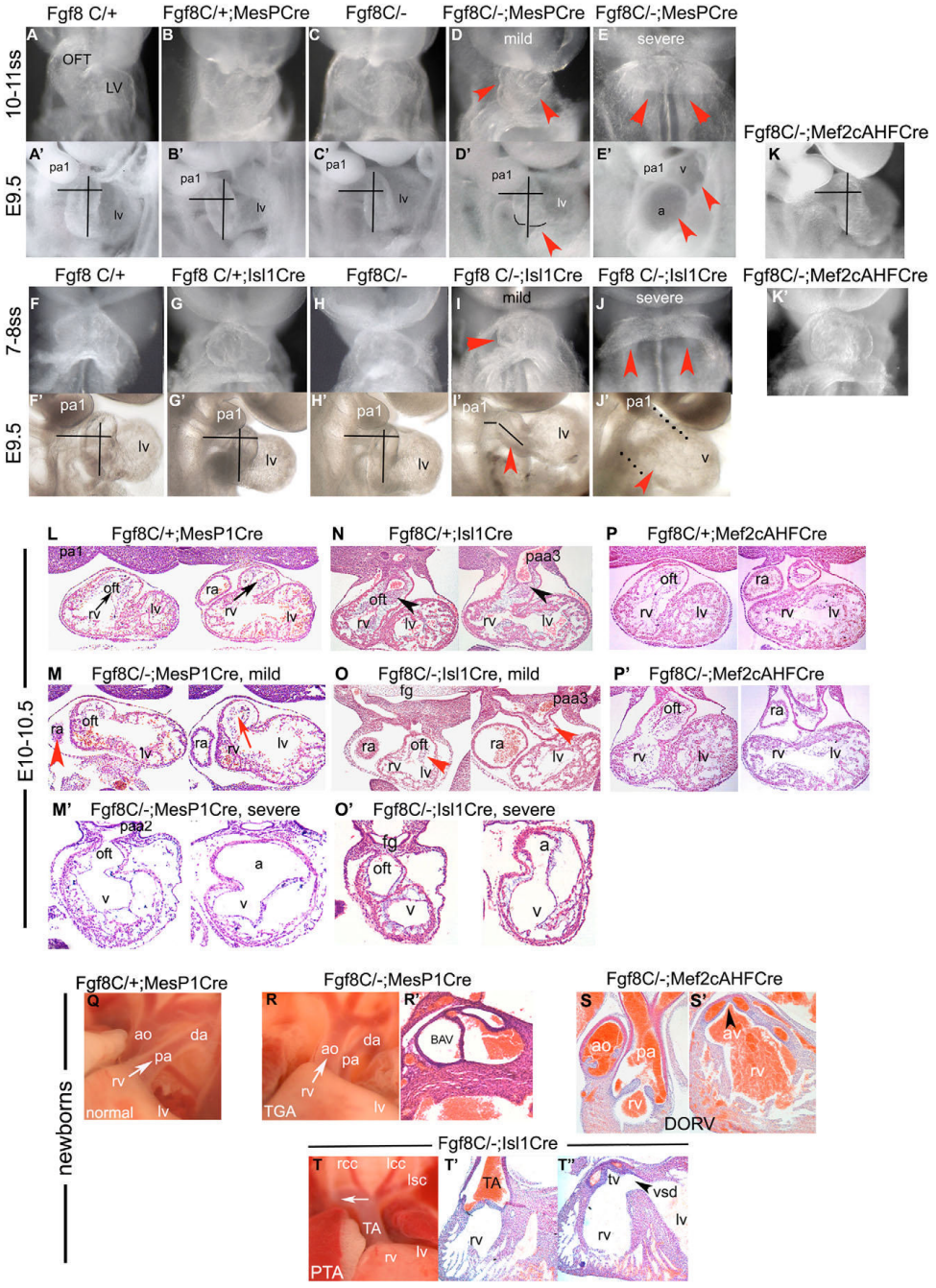

Fig. 2.

Ablation of Fgf8 in the cardiac crescent disrupts formation of the heart tube and outflow tract. (**A-E**) Ventral views of the 10-11ss *Fgf8;MesP1Cre* allelic series; genotypes are listed above. Heart tubes of $Fgf8^{C/-}$;$MesP1Cre^{/+}$ conditional mutants are small (red arrowheads). The mildly affected mutant heart (D) is looping, but all segments are small. Although the severely affected mutant (E) has 10 somites, its heart is the size of the 4-5ss control. Note the normal morphology of $Fgf8^{C/+}$;$MesP1Cre^{/+}$(B) and $Fgf8^{C/-}$(C). (**A′-E′**) Right lateral views of the E9.5 *Fgf8;MesP1Cre* allelic series. Superimposed black lines are the same length in each panel. The mildly affected mutant (D′) has a short, narrow OFT and a small RV (black outline, red arrowhead). (E′) The severely affected mutant has a single dilated ventricle, an incompletely

looped heart and no OFT (red arrowheads). (**F-J**) Ventral views of the 7-8ss *Fgf8;Isl1Cre* allelic series. *Fgf8*$^{C/+}$;*Isl1*$^{Cre/+}$(G) is normal, whereas the accruing RV/OFT of the mildly affected *Fgf8*$^{C/-}$;*Isl1*$^{Cre/+}$ mutant (I) is small (red arrowhead, this phenotype was not seen in >60 controls). (J) Severely affected *Fgf8;Isl1Cre* heart (red arrowheads). (**F′-J′**) Right lateral views of the *Fgf8;Isl1Cre* allelic series at E9.5. Black lines in panels F′-H′ are the same length and show normal flexion of the conotruncus/OFT. Mutant pharyngeal arches (pa) are hypoplastic (I′,J′). The mildly affected mutant (I′) has no visible RV and a short OFT lacking normal flexion (black lines); the OFT arises from the LV. Severely affected mutants (J′) have incompletely looped, dilated hearts. (**K**,**K′**) *Fgf8;Mef2cAHFCre* mutants at E9.5 and 8ss appear normal. (**L**) Sectioned E10.0 *Fgf8*$^{C/+}$;*MesP1Cre*$^{/+}$ control. The OFT arises from the RV (black arrows). (**M**) Sectioned mild E10.0 *Fgf8*$^{C/-}$;*MesP1Cre*$^{/+}$ mutant heart with a short OFT and small RV. The OFT arises abnormally from the LV (red arrow). Note the enlarged right atrium (ra, red arrowhead) and small RV. OFT cushion cellularity appears normal. (**M′**) Sectioned, severe/dying *Fgf8*$^{C/-}$;*MesP1Cre*$^{/+}$ mutant; the single ventricle (v), short OFT, and atrium (a) are all dilated. No RV is present. (**N**) Sectioned E10.5 *Fgf8*$^{C/+}$;*Isl1*$^{Cre/+}$ control. The OFT arises from the RV and is beginning to septate; the conotruncal cushions are dense with mesenchymal cells (black arrowheads). (**O**) Sectioned, mild E10.5 *Fgf8*$^{C/-}$;*Isl1*$^{Cre/+}$ mutant with a RA enlargement, RV hypoplasia, and the OFT arising from the LV. OFT cushions are hypocellular (red arrowheads). (**O′**) Sectioned, severe E10.5 *Fgf8*$^{C/-}$;*Isl1*$^{Cre/+}$ mutant. There is a dilated single ventricle and atrium. (**P**) *Fgf8*$^{C/+}$;*Mef2cAHFCre*control. (**P′**) Sectioned, E10.5 *Fgf8*$^{C/-}$ *;Mef2cAHFCre* mutants reveal normal OFT cushion cellularity and mild RV hypoplasia. (**Q**) Dissected heart/great vessels of a newborn *Fgf8*$^{C/+}$;*MesP1Cre*$^{/+}$ control. Great vessels are normally related (ao, aorta; pa, pulmonary artery; da, ductus arteriosus); white arrow indicates the normal RV alignment and egress via the pulmonary artery. The aorta is posterior and to the right of the pulmonary artery. (**R**) A newborn *Fgf8*$^{C/-}$;*MesP1Cre*$^{/+}$ mutant reveals TGA: abnormal OFT alignment/rotation with the aorta anterior, arising aberrantly from the RV (white arrow) and the pulmonary artery arising from the LV. (**R′**) Bicuspid aortic valve (BAV) in a *Fgf8*$^{C/-}$;*MesP1Cre*$^{/+}$ newborn. (**S**,**S′**) Aberrant OFT alignment/rotation in an *Fgf8*$^{C/-}$ *;Mef2cAHFCre* mutant manifest as DORV with both the aorta (av, aortic valve black arrowhead) and pulmonary artery arising from the RV. (**T**) Newborn *Fgf8*$^{C/-}$;*Isl1*$^{Cre/+}$ mutant with Persistent Truncus Arteriosus (PTA) and right aortic arch (white arrow). rcc, right common carotid artery; lcc, left common carotid artery; lsc, left subclavian artery; TA, truncus arteriosus. (**T′**,**T″**) Sectioned *Fgf8*$^{C/-}$;*Isl1*$^{Cre/+}$ mutant reveals an abnormally aligned truncal vessel completely overriding the RV; the LV egress is via a large ventricular septal defect (vsd, black arrowhead). tv, truncal valve.

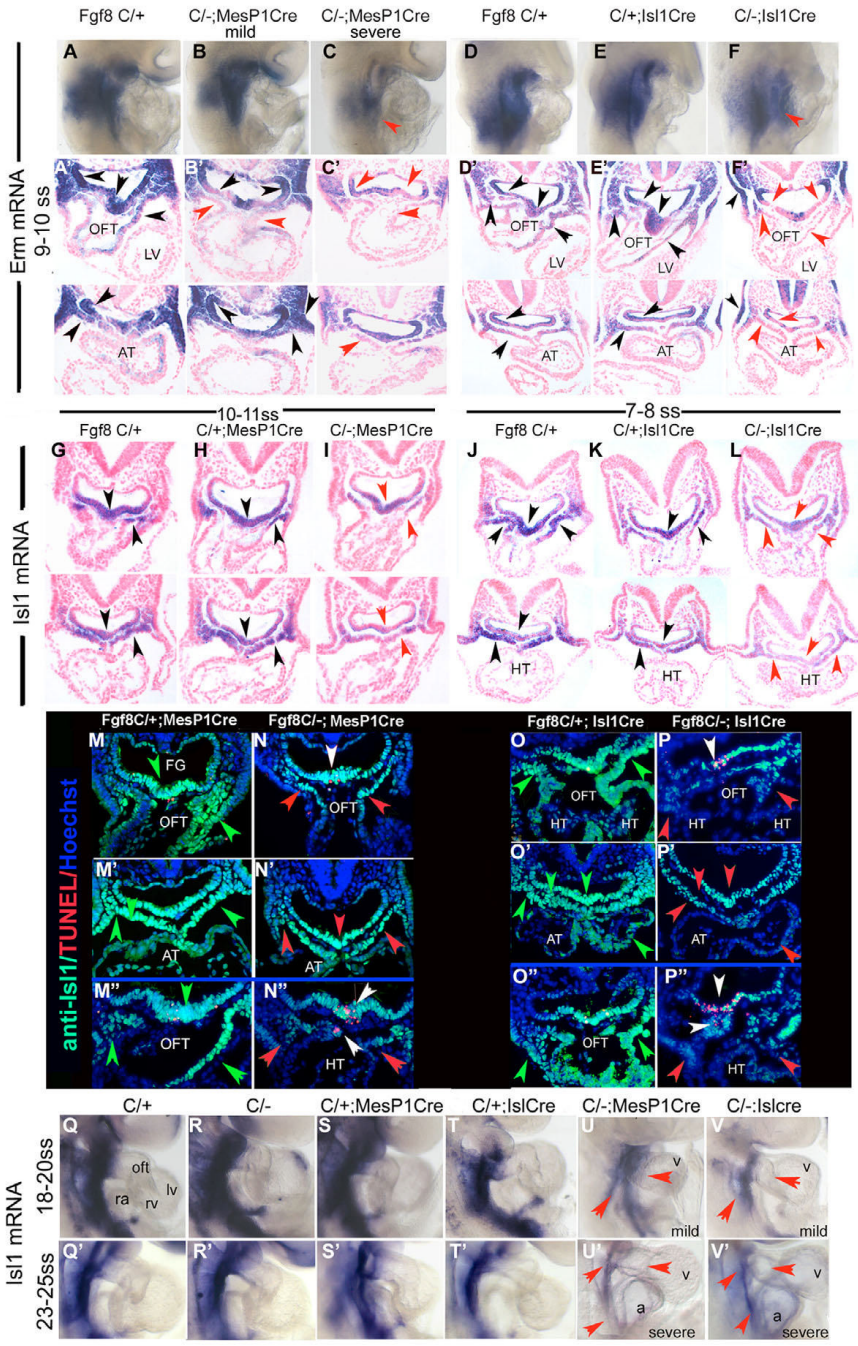

Fig. 3.

Loss of Fgf8 signaling disrupts *Erm*expression and Isl1 production in the anterior heart field. (**A**-**F**) Whole-mount (right lateral) 9-10ss embryos after in situ hybridization with an *Erm* antisense riboprobe. Genotypes are listed above each column; littermate controls processed with mutants are shown. Black arrowheads indicate the domains of normal *Erm* expression; red arrowheads indicate regions of decreased expression. (**A′**-**F′**) Upper row sections are anterior through the developing OFT/RV; bottom sections are at the level of the atrium (AT). (B′,C′) Two *Fgf8*$^{C/-}$;*MesP1Cre*$^{/+}$ mutants; the mild mutant (B′) has relatively normal Erm expression, but the severely affected mutant (C′) has decreased *Erm* in SM, OFT and ventral endoderm. (D′,E′) *Erm* expression is comparable in *Fgf8*$^{C/+}$;*Isl1*$^{+/+}$ and

Fgf8$^{C/+}$;*Isl1*$^{Cre/+}$ embryos. (F′) Severe *Fgf8*$^{C/-}$;*Isl1*$^{Cre/+}$ mutant with decreased *Erm* expression in ventral endoderm, SM and OFT. Note that endodermal expression is more severely affected than in the *Fgf8*$^{C/-}$;*MesP1Cre*$^{/+}$ mutants and that ectodermal expression remains intact. (**G-I**) *Isl1* mRNA in the 10ss MesP1Cre series; decreased *Isl1* expression is apparent in the mutant (red arrowheads). (**J-L**) *Isl1* mRNA in the 7ss Isl1Cre series; *Isl1* expression is markedly decreased in *Fgf8*$^{C/-}$;*Isl1*$^{Cre/+}$ mutants (L, red arrowheads) relative to *Fgf8* $^{C/+}$;*Isl1*$^{Cre/+}$ controls (K). (**M-P**″) Triple fluorescent immunohistochemistry detects Isl1 protein (green), apoptosis (TUNEL, red) and nuclei (Hoechst, blue). (M,M') Sections at the level of the OFT (M) and atrium (M') of a 10ss *Fgf8*$^{C/+}$;*MesP1Cre*$^{/+}$ control; endoderm, splanchnic and ventral pharyngeal mesoderm, and myocardial cells accumulating to the OFT stain intensely with anti-Isl1 antibody (green arrowheads). (N,N′) Same planes of section as above in an *Fgf8;MesP1Cre* mutant; the OFT is narrow and midline. The intensity of the Isl1 signal and the number of Isl1-positive (green) cells in the OFT and contiguous SM are decreased (red arrowheads). (M",N") Another 10ss control and mutant at the level of the OFT; this mutant has no OFT, no Isl1-positive cells in the heart tube (red arrowheads, HT) and excess apoptosis in the Isl1-positive endoderm and adjacent OFT (white arrowheads). (O,O′) 8ss *Fgf8*$^{C/+}$;*Isl1*$^{Cre/+}$ control; at this stage, the OFT is just beginning to accrue and stains with Isl1 (green arrowheads). (P,P′) *Fgf8*$^{C/-}$;*Isl1*$^{Cre/+}$ mutant. Note the excess apoptosis in the Isl1-positive endoderm (white arrowhead). The OFT is abnormally short and few Isl1-positive cells are present in the SM, HT or atrium (red arrowheads). (O",P") The alterations in Isl1 protein are reproducible in another 8ss *Fgf8*$^{C/+}$;*Isl1*$^{Cre/+}$ control and *Fgf8*$^{C/-}$;*Isl1*$^{Cre/+}$ mutant; the mutant has few Isl1-positive cells in the HT (red arrowheads) and excess apoptosis in endoderm (white arrowhead). (**Q-V**′) Right lateral views of the pharynx/heart of embryos assayed for *Isl1* mRNA. Genotypes are listed above, somite stages at the left. The level of *Isl1* mRNA (red arrowheads) correlates with the severity of the cardiac/OFT phenotype in mutants.

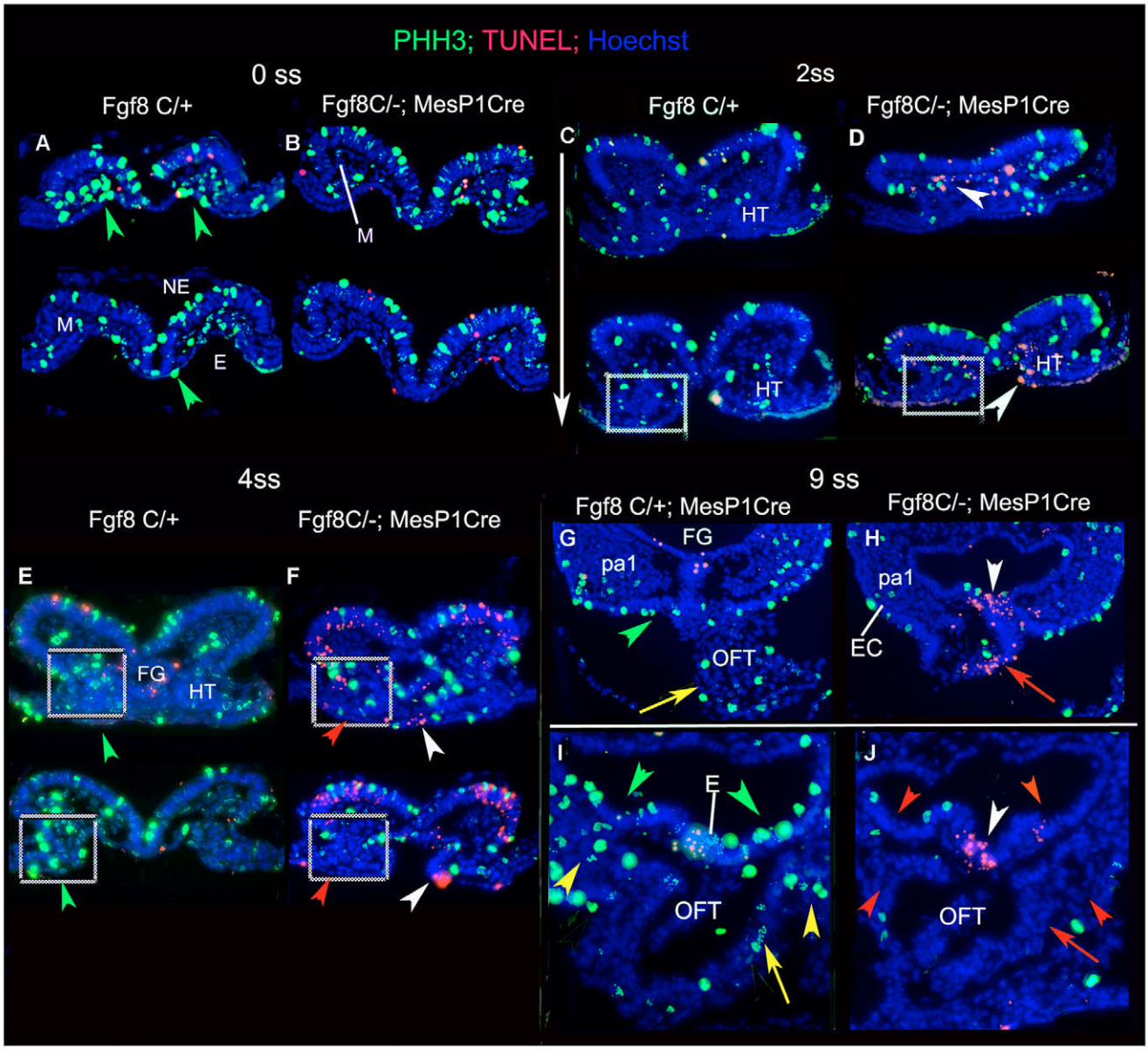

Fig. 4.

Ablation of *Fgf8* in crescent mesoderm increases apoptosis and decreases proliferation in foregut endoderm and AHF mesoderm. Transverse cryosectioned *Fgf8;MesP1Cre* mutants/controls stained with anti-PHH3 (green, mitotic cells) and Hoechst (nuclei), and for apoptosis (TUNEL, red). Sections proceed anterior (top) to posterior (bottom), indicated by the white arrow. (**A**,**B**) 0ss; abundant proliferation and minimal apoptosis are detected in control mesoderm (M), endoderm (E) and neuroectoderm (NE) (A, green arrowheads). The number of proliferating cells in the mutant (B) mesoderm appears to be decreased. (**C**,**D**) 2ss; increased apoptosis in mutant (D) endoderm (white arrowheads). (**E**,**F**) 4ss; increased apoptosis in mutant endoderm (white arrowheads). Many cells are proliferating in the control heart tube mesoderm (HT, white box, green arrowheads) but only a few in the mutant (red arrowheads). (**G-J**) 9ss; excess apoptosis in the midline endoderm (white arrowheads) and developing OFT of mutants (H,J, red arrows; see also Fig. 3N",P"). More proliferating cells are detected in the pharyngeal epithelia (green arrowheads; EC, ectoderm; E, endoderm), SM (yellow arrowheads) and

contiguous OFT (yellow arrows) of control. Posterior sections in panels I and J are at twice the magnification of those in G and H. pa1, pharyngeal arch 1.

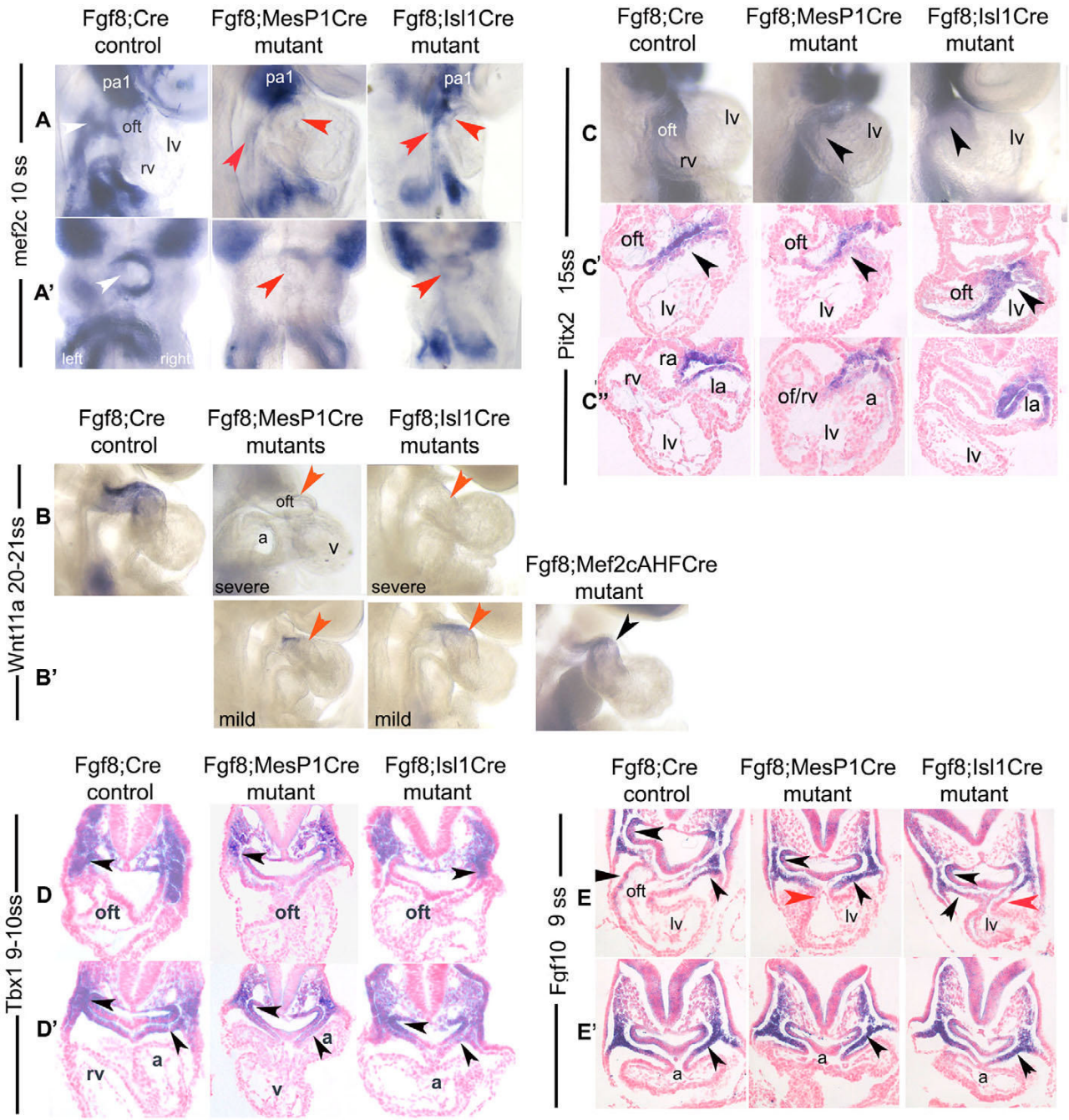

Fig. 5.

Loss of Fgf8 specifically disrupts the Isl1/Mef2c pathway in the AHF. In situ hybridized embryos; genotypes listed at the top, riboprobe and somite stage at the left. (**A**) *Mef2c* in 10ss embryos; right lateral view, red arrowheads indicate decreased signal in the OFT and AHF/SM of mutants. (**A′**) Dorsal views; the ring of staining around the nascent OFT is markedly less intense in the mutants (red arrowheads). (**B**,**B′**) *Wnt11* at 20-21ss; close up of right side of the heart. Note the undetectable signal in the OFT myocardium of severe mutants (red arrowheads), and decreased levels in the mild variants (B'); expression is intact in *Fgf8*$^{C/-}$ *;Mef2cAHFCre* mutants (black arrowhead). (**C-C″**) *Pitx2* at 15ss; right lateral views in C, transverse sections in C′,C″. Upper panels are at the level of the OFT, lower panels at

level of the atrium/sinus venosus. (**D**,**D′**) *Tbx1* expression in transverse-sectioned 9-10ss embryos appears normal in the endoderm and SM/AHF. (**E**,**E′**) *Fgf10* in transverse-sectioned 8ss embryos. Expression is intact (black arowheads) except in mutant proximal OFT myocardium (red arrowheads).

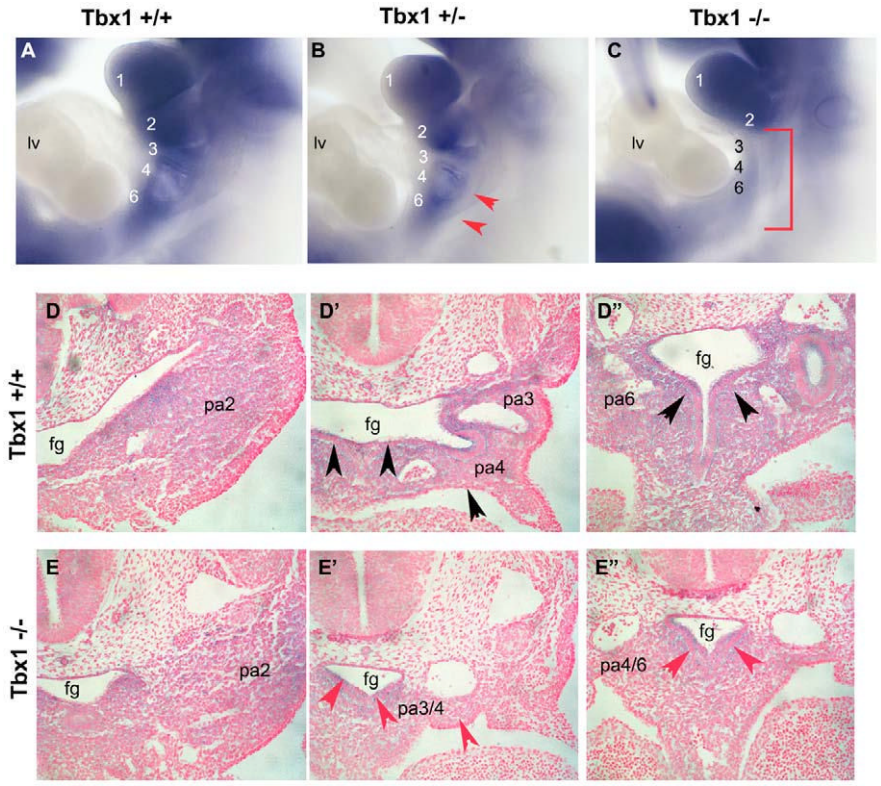

Fig. 6.

Loss of *Tbx1*function specifically disrupts the expression of Fgf receptor 1 in the caudal pharyngeal arches. (**A-C**) Whole-mount in situ hybridized 35ss embryos of the indicated genotypes. Note the *Tbx1* dose-dependent reduction in Fgfr1 expression in arches 3-6 (red arrowheads and bracket), and the preserved expression in arches 1 and 2, and the limb bud. This finding was consistent in 6/6 heterozygotes and mutants assayed. (**D-E**″) Sections reveal decreased *Fgfr1* expression in unsegmented endoderm/mesenchyme of the mutant (red arrowheads) compared with the control (black arrowheads).

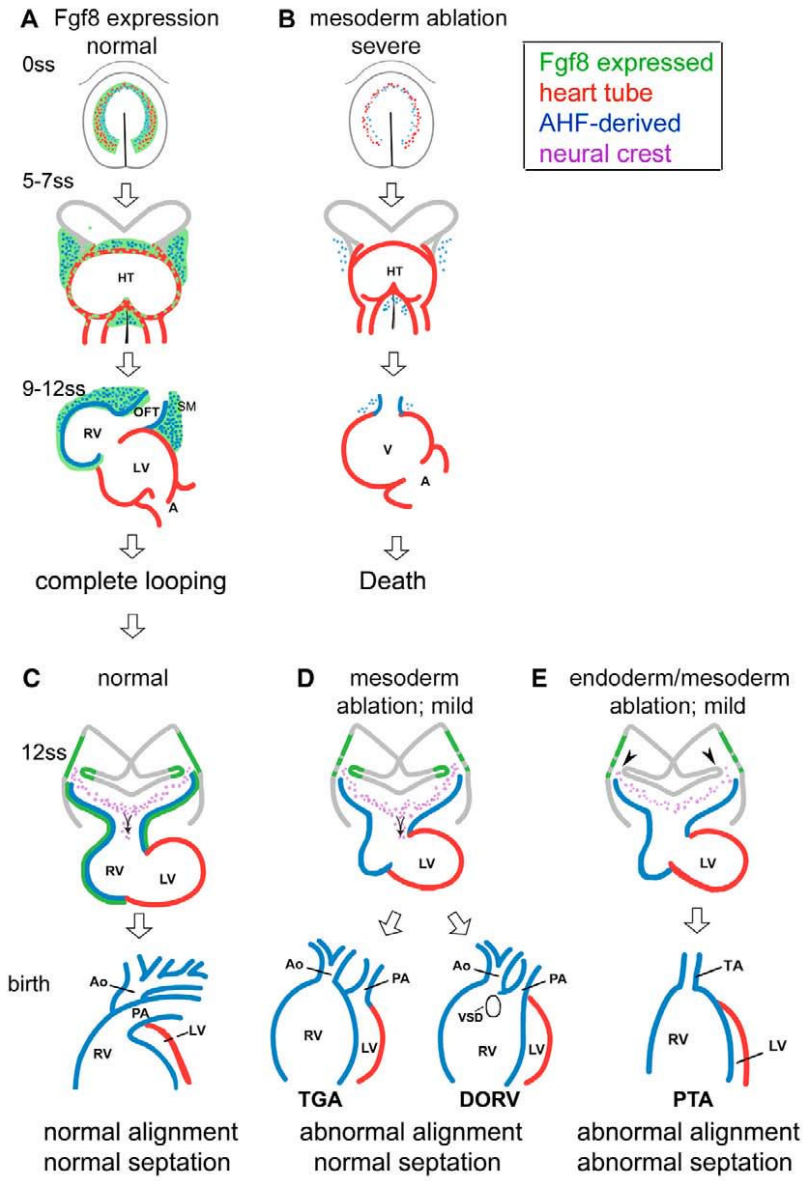

Fig. 7.

Schematics illustrating cardiovascular phenotypes resulting from the differential ablation of *Fgf8*. (**A**) Normal Fgf8 expression (green denotes normal *Fgf8* expression domains)**.** (**B**) Ablation of *Fgf8* in mesodermal precursors of the heart tube (red) and AHF (blue) at the crescent/early somite stages generates small heart tubes and prevents accrual of the RV/OFT myocardium, usually causing death. (**C-E**) Compared with wild type (C), loss of mesodermal Fgf8 in surviving *Fgf8;MesP1Cre* mutants and in *Fgf8;Mef2cAHFCre* mutants disrupts OFT alignment resulting in TGA and DORV (D). Absence of *Fgf8* in the endoderm and mesoderm disrupts septation and alignment, respectively, resulting in PTA with an abnormally aligned truncal vessel (E).